Background and Photoexcited Carrier Dependence of Terahertz Radiation from Mg-Doped Nonpolar Indium Nitride Films

2010 Appl. Phys. Express 3 122105

(http://iopscience.iop.org/1882-0786/3/12/122105)

Background and Photoexcited Carrier Dependence of Terahertz Radiation from Mg-Doped Nonpolar Indium Nitride Films

Hyeyoung Ahn*, Yi-Jou Yeh, Yu-Liang Hong[1], and Shangjr Gwo[1]

Department of Photonics and Institute of Electro-Optical Engineering, National Chiao Tung University, Hsinchu, Taiwan 30010, R.O.C.
[1]*Department of Physics, National Tsing Hua University, Hsinchu, Taiwan 30013, R.O.C.*

Received October 22, 2010; accepted November 13, 2010; published online December 3, 2010

We report terahertz (THz) generation from Mg-doped nonpolar (*a*-plane) InN (*a*-InN:Mg). While the amplitude and polarity of the THz field from Mg-doped polar (*c*-plane) InN depend on the background carrier density, the p-polarized THz field from *a*-InN:Mg has background carrier-insensitive intensity and polarity, which can be attributed to carrier transport in a polarization-induced in-plane electric field. A small but apparent azimuthal angle dependence of the THz field from *a*-InN:Mg shows the additional contribution of the second-order nonlinear optical effect. Meanwhile, in this study, we did not observe the contribution of the intrinsic in-plane electric field which is significant for high stacking fault density nonpolar InN.

DOI: 10.1143/APEX.3.122105

Since the discovery of its narrow intrinsic band gap, indium nitride (InN) has received much attention in terahertz (THz) range applications due to its high electron mobility and low interband absorption. Because of its large electron affinity, however, as-grown InN film is typically n-type and has an extremely high background carrier density ($n \sim 10^{17}$–$10^{18}\,\mathrm{cm}^{-3}$). For semiconductors with a high background carrier density, THz emission can be seriously limited by the strong screening of the photo-Dember field.[1,2] Therefore, THz emission from as-grown *c*-plane InN (*c*-InN) is typically much weaker than that from other semiconductors, such as InAs[3–6] and the reduction of THz intensity with the increase of the carrier density has been observed for as-grown and Si-doped InN.[7] In our recent work, we have demonstrated drastically enhanced THz radiation from magnesium (Mg) doped *c*-InN, in which Mg works as an acceptor dopant to reduce the background carrier density.[8] However, the increase of Mg doping in InN films is often accompanied by inferior crystalline quality.[9] In addition, the surge current-induced THz radiation from *c*-InN critically suffers from a low light-extraction problem due to the large total internal reflection occurring within a material of high refractive index.[10]

As an effort to increase the light extraction from InN, we have studied THz generation from InN films grown along the *a*-axis (*a*-InN) and found that THz generation from *a*-InN is dominated by the polarization-induced in-plane electric field combined with an optical nonlinear effect.[11] THz signal induced by in-plane dipole oscillation can be favorably coupled to a narrow emission cone and its magnitude can surpass that of the surge-current-induced THz radiation. The intensity enhancement as much as two orders of magnitude from *a*-InN is comparable or even larger than the enhancement achieved by applying an external magnetic field parallel to the semiconductor surface.[12–14] Meanwhile, for nonpolar (*a*- and *m*-plane) InN photoexcited at a lower excitation fluence ($\sim\mu\mathrm{J/cm}^2$), Metcalfe *et al.* proposed another emission mechanism which is attributed to the drift of carriers in an intrinsic in-plane electric field.[15] In this mechanism, the intrinsic in-plane electric field is induced by the high-density stacking fault of nonpolar InN along the *c*-axis and shows a sinusoidal azimuthal dependence on sample rotation. Moreover, the relatively weak angular independent component of THz signals has been suggested to be due to the photo-Dember effect.

THz generation associated with the photo-Dember effect is closely dependent on the background carrier density as well as the photoexcited carrier density. Therefore, the controversy of the THz generation mechanism of *a*-InN can be clarified by investigating the carrier density dependence of THz radiation, including both the background and photoexcited carriers. In this paper, we present THz emission from the *a*-InN films doped with Mg (*a*-InN:Mg). Several *a*-InN:Mg films with various background carrier densities were prepared by growing the samples at different Mg cell temperatures and the carrier density dependent THz generation is compared with that from *c*-InN:Mg. We have also measured THz generation from *a*-InN:Mg excited at different pump fluences and its dependence on the azimuthal sample rotation. In sharp contrast to the *c*-InN:Mg case, THz emissions from the *a*-InN:Mg films with different background carrier densities are comparable to that from undoped *a*-InN, and more importantly, do not decrease with the increase of carrier density, indicating the negligible contribution of the photo-Dember effect to THz generation from *a*-InN:Mg.

For this work, several *a*-InN and *a*-InN:Mg films (with a nominal thickness of $\sim$1.2 μm) were grown on *r*-plane $\{1\bar{1}02\}$ sapphire substrates, whereas $-c$-plane $(000\bar{1})$ undoped and Mg-doped InN films with a thicknesses of $\sim$1.2 μm were grown on Si(111) substrates by plasma-assisted molecular beam epitaxy. Mg doping was performed with a high-purity Mg (6N) Knudsen cell and the Mg doping level was controlled by regulating the cell temperature between 180 and 290 °C. The electron density and mobility of the undoped *a*-InN film determined by room-temperature electron Hall effect measurement are $\sim 7 \times 10^{18}\,\mathrm{cm}^{-3}$ and $300\,\mathrm{cm}^2\,\mathrm{V}^{-1}\,\mathrm{s}^{-1}$, respectively. Those of *c*-InN:Mg and *a*-InN:Mg are subject to the Mg doping level and their dependence on the Mg cell temperature is illustrated in Fig. 1. In this figure, the carrier density and electron mobility at a Mg cell temperature of 0 °C correspond to those of undoped *c*- and *a*-InN films. Here, the carrier density shows a peculiar V-shape dependence on the Mg doping level in such a way that the carrier density first decreases as the Mg cell temperature increases and then increases at higher Mg cell temperatures due to strong longitudinal optical phonon–plasmon coupling.[16] For

*E-mail address: hyahn@mail.nctu.edu.tw

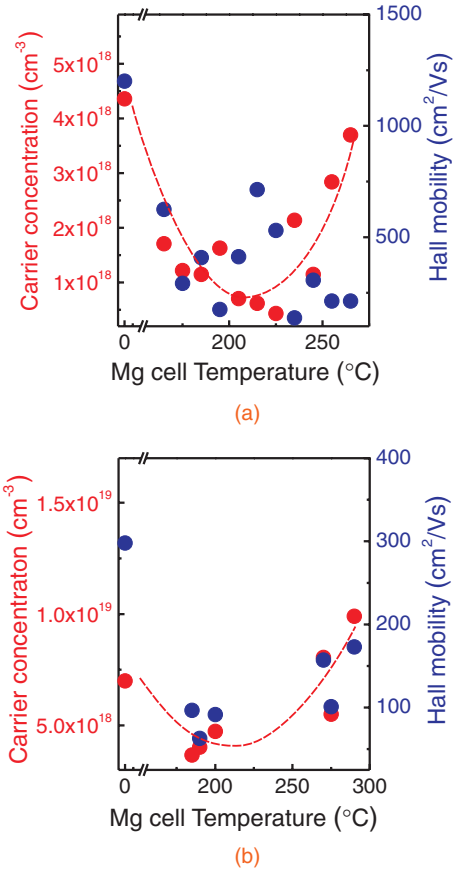

Fig. 1. Carrier density and Hall mobility of (a) *c*- and (b) *a*-InN:Mg as a function of Mg cell temperature. V-shape dependence of carrier concentration can be observed for both samples.

a-InN:Mg doped at Mg cell temperatures $>250\,^{\circ}$C, the carrier density can be even higher than that of undoped *a*-InN. THz emission measurements were performed using a Ti:sapphire laser system, which delivers $\sim$50 fs optical pulses at a center wavelength of 800 nm with a repetition rate of 1 kHz. THz pulses were detected by the free-space electro-optic sampling method in a 2-mm-thick ZnTe crystal as a function of delay time with respect to the optical pump pulse. The typical fluence of pump pulses incident at 70° was $\sim$240 μJ/cm^2. The experimental details of time-domain THz emission measurement can be found elsewhere.[17)]

Figure 2 shows the peak amplitude of p-polarized THz radiation from *a*- and *c*-InN:Mg films as a function of background carrier density. For *c*-InN:Mg, THz emission is sharply enhanced as n decreases and the THz amplitude from *c*-InN:Mg with $n_c \sim 1 \times 10^{18}\,\mathrm{cm}^{-3}$ is as strong as that from an n-type InAs (100) film with $n \sim 10^{17}\,\mathrm{cm}^{-3}$ (shown by a triangle symbol). With the carrier density below n_c, the THz amplitude begins to decrease again and its polarity changes to a negative sign. As is well known, THz generation associated with the surge current depends on the densities of both background and photoexcited carriers through the relation[18)] $J = J_E + J_D = eE(n_t\mu_n + p_t\mu_p) + e(D_n\nabla n_t - D_p\nabla p_t)$, where n_t (p_t) includes both background carriers and photoexcited carriers, and μ_n (μ_p) and D_n (D_p) correspond to the mobility and diffusion coefficient of electrons (holes), respectively. The fast decay of THz signals

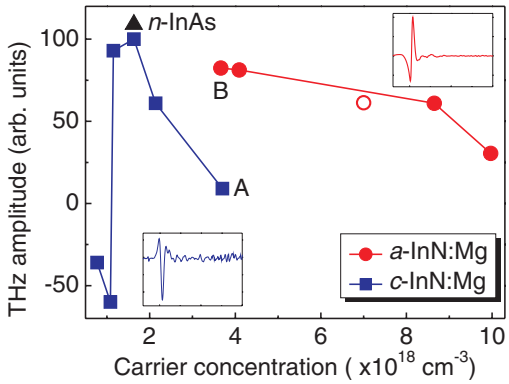

Fig. 2. Peak amplitudes of the THz radiation from Mg-doped *c*- (squares) and *a*-InN (circles) films as a function of background carrier concentration. The open circle indicates the peak amplitude obtained from an undoped *a*-InN and the solid triangle corresponds to an n-type InAs (100) with a carrier density of $\sim 2 \times 10^{17}\,\mathrm{cm}^{-3}$. The two insets in the figure illustrate the waveforms of THz radiation with positive and negative polarities, respectively.

from *c*-InN:Mg with the increase of the background carrier density and the flip of the polarity indicates the interplay of the diffusion and drift currents, which direct the outward and inward directions of the InN film, respectively.[8)]

The carrier density dependence of THz radiation of *a*-InN:Mg shown in Fig. 2 is different from that of *c*-InN:Mg in several ways. First, the amplitude of the THz field from *a*-InN:Mg is as high as that from an undoped *a*-InN (shown by an open circle in Fig. 2) and it keeps the similarly high amplitude even when the carrier density is increased to about $1 \times 10^{19}\,\mathrm{cm}^{-3}$. Second, the polarity of THz signals from *a*-InN:Mg is positive (parallel to the polarity of an n-type GaAs[8)]) and no polarity flipping is observed.

In order to measure the contribution of the surge current to the THz generation from *a*-InN:Mg, we compared THz signals from *c*-InN:Mg (sample A) and *a*-InN:Mg (sample B) films with a similar background carrier density $\sim 3.5 \times 10^{18}\,\mathrm{cm}^{-3}$. Since each sample in Fig. 2 is excited at the same pump fluence, samples A and B also have the same photoexcited carrier density. Therefore the surge-current-induced THz generation from samples A and B with the same background and photoexcited carrier densities should be of the same order. However, Fig. 2 shows that the THz signal from sample B is at least ten times (100 times in intensity) stronger than that from sample A, providing clear evidence that contribution of the surge current to THz generation from *a*-InN:Mg is negligible. We attribute the major THz generation mechanism of *a*-InN:Mg to carrier transport in an in-plane electric field, the same as that of an undoped *a*-InN. Since the in-plane electric field is due to the anisotropic charge distribution between In and N atoms in a basal plane, THz generation from *a*-InN:Mg would depend on the density of In–N pairs instead of the background charge carriers. The slight decrease of THz amplitude with the increase of the carrier density may be due to the crystal quality deterioration, which is accompanied by the decrease of the intensity of near-infrared photoluminescence (not shown).

Typically, the optical rectification mechanism is important for the highly excited samples and the main characteristic

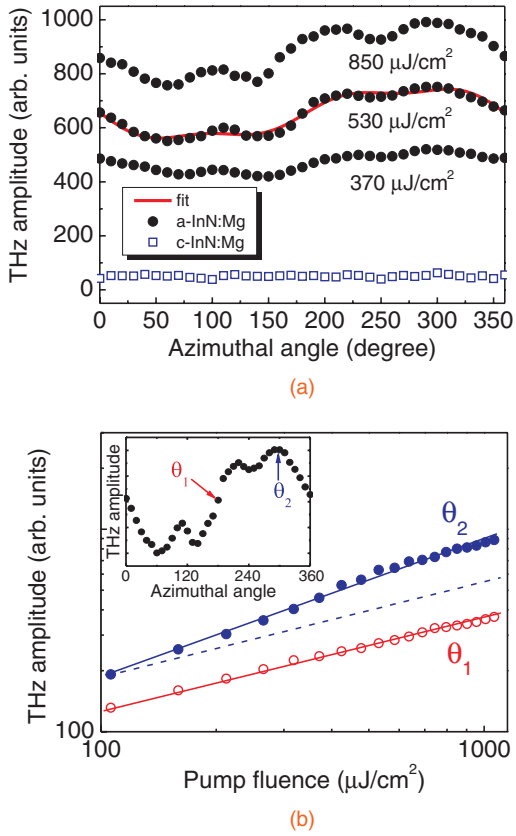

Fig. 3. (a) Azimuthal angle dependence of THz radiation from *a*-InN:Mg measured at different excitation fluences. The solid line is obtained by an analysis of the bulk and surface second-order susceptibility tensor elements of *a*-InN.[11] (b) The amplitudes of the THz field measured at the azimuthal angles θ_1 and θ_2 as a function of pump fluence.

property of the optical rectification mechanism distinguishing it from the current surge mechanisms is the azimuthal anisotropy. Figure 3 shows the p-polarized THz amplitude from *a*-InN:Mg as a function of azimuthal rotation angle θ of the sample. THz signals from *a*-InN:Mg show a similar angular dependence to that from undoped *a*-InN,[11] whereas that of *c*-InN:Mg is angular independent. Figure 3(a) shows that the angular-dependent component becomes more significant as the pump fluence is increased. In order to isolate the angular dependent component from the angular-independent one, we measured the THz amplitudes at two azimuthal angles θ_1 and θ_2, where the angular modulation of THz field is zero and maximum, respectively. Figure 3(b) shows that the THz radiation measured at θ_2 increases faster than that at θ_1 as the pump fluence is increased. The linear increase of THz radiation measured at θ_1 is due to the increase of photoexcited carriers, while the larger linear slope of terahertz radiation at θ_2 indicates that a nonlinear optical effect contribution becomes more pronounced as the pump fluence is increased. This result is different from the simple $\sin\theta$ dependence of the THz field reported by Metcalfe *et al.*[14] for nonpolar InN films excited at a low fluence ($1-50\,\mu J/cm^2$). The $\sin\theta$ dependence is due to a stacking fault-terminated internal polarization at wurzite domain boundaries parallel to the *c*-axis. The same authors have also reported that a similar $\sin\theta$ dependence can be observed for a nonpolar GaN film with a high stacking-fault density and the samples with a low stacking-fault density do not show the azimuthal angle dependence.[19] For *a*-InN:Mg films, we found that the angular-dependent component in Fig. 3 becomes barely detectable when the pump fluence is reduced to $<100\,\mu J/cm^2$, indicating that our *a*-InN:Mg films are not affected by stacking fault.

In summary, we have investigated the background carrier density dependence and azimuthal angle dependence of THz emission from the *a*-InN:Mg films. Intense THz amplitudes with a positive polarity from *a*-InN:Mg are nearly independent of the background carrier density, indicating the negligible contribution of the surge current. The THz generation mechanism from *a*-InN:Mg consists of carrier transport in the in-plane electric field and the second-order nonlinear optical effect, which are not governed by the background carrier density, but by the crystal structure and symmetry.

Acknowledgments This work was supported by the National Science Council (NSC 98-2112-M-009-009-MY3) and the National Nanoscience and Nanotechnology Project (NSC 98-2120-M-007-009) in Taiwan.

1) K. Liu, J. Xu, T. Yuan, and X.-C. Zhang: Phys. Rev. B **73** (2006) 155330.
2) R. Ascazubi, C. Shneider, I. Wilke, R. Pino, and P. S. Dutta: Phys. Rev. B **72** (2005) 045328.
3) H. Ahn, Y.-P. Ku, Y.-C. Wang, C.-H. Chuang, S. Gwo, and C.-L. Pan: Appl. Phys. Lett. **91** (2007) 132108.
4) I. Wilke, R. Ascazubi, H. Lu, and W. J. Schaff: Appl. Phys. Lett. **93** (2008) 221113.
5) G. D. Chern, E. D. Readinger, H. Shen, M. Wraback, C. S. Gallinat, G. Koblmüller, and J. S. Speck: Appl. Phys. Lett. **89** (2006) 141115.
6) R. Acsazubi, I. Wilke, K. Denniston, H. L. Lu, and W. J. Schaff: Appl. Phys. Lett. **84** (2004) 4810.
7) R. Ascazubi, I. Wilke, S. Cho, H. Lu, and W. J. Schaff: Appl. Phys. Lett. **88** (2006) 112111.
8) H. Ahn, Y.-J. Yeh, Y.-L. Hong, and S. Gwo: Appl. Phys. Lett. **95** (2009) 232104.
9) W. Walukiewicz, J. W. Ager III, K. M. Yu, Z. Liliental-Weber, J. Wu, S. X. Li, R. E. Jones, and J. D. Denlinger: J. Phys. D **39** (2006) R83.
10) M. B. Johnston, D. M. Whittaker, A. Corchia, A. G. Davies, and E. H. Linfield: Phys. Rev. B **65** (2002) 165301.
11) H. Ahn, Y.-P. Ku, C.-H. Chuang, C.-L. Pan, H.-W. Lin, Y.-L. Hong, and S. Gwo: Appl. Phys. Lett. **92** (2008) 102103.
12) X. C. Zhang, Y. Liu, T. D. Hewitt, T. Sangsiri, L. E. Kingsley, and M. Weiner: Appl. Phys. Lett. **62** (1993) 2003.
13) P. Gu, M. Tani, S. Kono, K. Sakai, and X. C. Zhang: J. Appl. Phys. **91** (2002) 5533.
14) S. C. Howells, S. D. Herrera, and L. A. Schlie: Appl. Phys. Lett. **65** (1994) 2946.
15) G. D. Metcalfe, H. Shen, M. Wraback, G. Koblmüller, C. Gallinat, F. Wu, and J. S. Speck: Appl. Phys. Express. **3** (2010) 092201.
16) M. Fujiwara, Y. Ishihiro, X. Wang, S.-B. Che, and A. Yoshikawa: Appl. Phys. Lett. **93** (2008) 231903.
17) H. Ahn, C.-L. Pan, and S. Gwo: Proc. SPIE **7216** (2009) 72160T.
18) J. N. Heyman, N. Coates, and A. Reinhardt: Appl. Phys. Lett. **83** (2003) 5476.
19) G. D. Metcalfe, H. Shen, M. Wraback, A. Hirai, F. Wu, and J. S. Speck: Appl. Phys. Lett. **92** (2008) 241106.